THE JOURNAL OF PHYSICAL CHEMISTRY B

pubs.acs.org/JPCB Article

Revealing the Origin of the Specificity of Calcium and Sodium Cations Binding to Adsorption Monolayers of Two Anionic Surfactants

Fatmegyul Mustan, Anela Ivanova,* Slavka Tcholakova, and Nikolai Denkov

Cite This: J. Phys. Chem. B 2020, 124, 10514−10528 Read Online

ACCESS | Metrics & More | Article Recommendations | Supporting Information

ABSTRACT: The studied anionic surfactants linear alkyl benzene sulfonate (LAS) and sodium lauryl ether sulfate (SLES) are widely used key ingredients in many home and personal care products. These two surfactants are known to react very differently with multivalent counterions, including Ca^{2+}. This is explained by a stronger interaction of the calcium cation with the LAS molecules, compared to SLES. The molecular origin of this difference in the interactions remains unclear. In the current study, we conduct classical atomistic molecular dynamics simulations to compare the ion interactions with the adsorption layers of these two surfactants, formed at the vacuum−water interface. Trajectories of 150 ns are generated to characterize the adsorption layer structure and the binding of Na^+ and Ca^{2+} ions. We found that both surfactants behave similarly in the presence of Na^+ ions. However, when Ca^{2+} is added, Na^+ ions are completely displaced from the surface with adsorbed LAS molecules, while this displacement occurs only partially for SLES. The simulations show that the preference of Ca^{2+} to the LAS molecules is due to a strong specific attraction with the sulfonate head-group, besides the electrostatic one. This specific attraction involves significant reduction of the hydration shells of the interacting calcium cation and sulfonate group, which couple directly and form surface clusters of LAS molecules, coordinated around the adsorbed Ca^{2+} ions. In contrast, SLES molecules do not exhibit such specific interaction because the hydration shell around the sulfate anion is more stable, due to the extra oxygen atom in the sulfate group, thus precluding substantial dehydration and direct coupling with any of the cations studied.

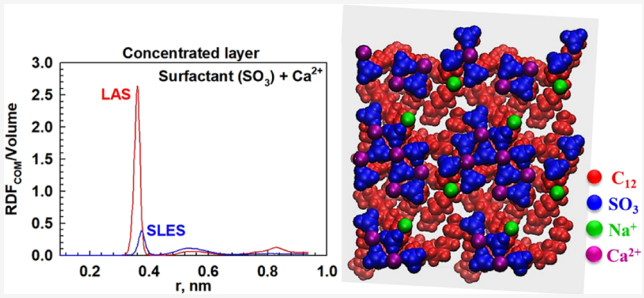

INTRODUCTION

Surfactants play a key role in the stabilization of various colloid systems used in industry, by adsorbing at different interfaces. The two anionic surfactants studied in this article, linear alkyl benzene sulfonate (LAS) and sodium lauryl ether sulfate (SLES), are used in innumerable detergent formulations for home and personal care.[1−6] The optimization of the various detergent preparations requires understanding of their behavior in electrolyte solutions, containing several cations. Most often, Ca^{2+} and Mg^{2+} of millimolar concentrations come from tap water, while Na^+ ions are usually added in the commercial liquid detergent formulations to adjust their viscosity. Therefore, understanding the interactions of LAS and SLES with Na^+ and divalent counterions, such as Ca^{2+} and Mg^{2+}, is of primary importance in this area. The interaction of LAS with Ca^{2+} ions is of particular interest.

Experimental studies of the effect of divalent counterions on the surface properties of LAS and SLES showed that the addition of Ca^{2+} to LAS solutions leads to extensive surfactant precipitation, even at very low calcium concentrations, due to the formation of water-insoluble calcium-LAS salt,[7] while no such effect is observed for SLES. Surfactant−counterion interaction could be quantified by the ion-binding energy to the surfactant molecules. With this aim in view, the standard free energy of counterion binding from aqueous solutions to surfactant adsorption layers was evaluated from surface tension isotherms.[5,6] The authors found that the interaction between Na^+ and LAS is purely electrostatic and the nonelectrostatic component of the adsorption energy is rather small: $\Delta\mu_{Na}^{0} < 0.1kT$ (where kT is the thermal energy), whereas Ca^{2+} has very high specific binding energy to LAS—the specific nonelectrostatic adsorption energy share is $\Delta\mu_{Ca}^{0} \approx 3.5kT$. The reason for this large difference in the ion−surfactant interactions for these two cations is unclear at present. Molecular dynamics (MD) is a particularly powerful tool to analyze such phenomena and to clarify their origin at the molecular and atomistic levels.

In the last two decades, MD simulations have been widely used to study the behavior of amphiphilic molecules in the

Received: July 21, 2020
Revised: October 2, 2020
Published: November 4, 2020

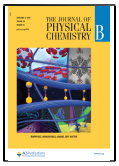

https://dx.doi.org/10.1021/acs.jpcb.0c06649
J. Phys. Chem. B 2020, 124, 10514−10528

bulk and at interfaces. The structure and dynamics of surfactant layers formed at the vacuum−water[8−17] and oil−water[18−21] interfaces is characterized using atomistic or coarse-grained[22,23] MD simulations. Almost all reported molecular models are constructed by fixing the surfactant molecules at the interface at predefined areas per molecule. Most of the molecules studied at the air−water interface are ionic surfactants, such as the sodium dodecyl sulfate (SDS), sodium dodecyl sulfonate (SDSn), sodium dodecyl carboxylate (SDC), alkyl trimethylammonium bromide (C_{16}TAB or C_{12}TAB), or nonionic surfactants, e.g., different alkylether polyoxyethylenes (C_nEO_m).

Several studies of SLES[24,25] and LAS[26−32] were published, which reported atomistic MD simulations. For the sulfate type of molecules (sodium dodecyl sulfate and sodium dodecyl benzene sulfate), the influence of the presence of the ethylene oxide (EO) groups on the Ca^{2+} tolerance at the air−water interface was addressed in ref 24. The models consisted of two mirror-image monolayers with a total of 18 surfactant molecules (9 molecules in each layer), separated by water molecules and with 18 Na^+ and 9 Ca^{2+} ions added. The length of the periodic box edge was ≈3.2 nm. For all systems studied, 1 ns of MD trajectories was generated in ref 24 using the potential functions and parameters from the PCFF force field. The simulations showed that Ca^{2+} ions replace the Na^+ ions from the EO units in the SLES head-group. The EO groups may bind Ca^{2+}, leading to weakening of the interaction between the Ca^{2+} cation and the sulfate anion, which restrains the precipitation of the anionic surfactants. The observed effect is explained by the authors with the increased hydration of the sulfate ion, enhanced by the EO groups present in the molecules. In a separate work, Li et al.[25] studied alkylether sulfate with three EO groups. For this surfactant, a comparison between the interaction with Mg^{2+} and Ca^{2+} was made, aiming to explain the experimentally observed effect of the two cations on foam film stability. Atomistic MD simulations with 4 ns production runs were carried out using the COMPASS force field. The authors clarified that Mg^{2+} participates in the assembly of the surfactant molecules with its own hydration shell, which results in higher energy barriers of binding compared to Ca^{2+}. In contrast, aggregation of the surfactant molecules in the presence of Ca^{2+} was observed, and the authors suggested that this is the reason for the formation of unstable foam films due to the significant decrease in the hydration of Ca^{2+} bound to the surfactant heads.

LAS with 12 carbon atoms in the hydrophobic chain and a benzene ring bound at the sixth carbon atom was studied by Yang et al.[26] in comparison to SDS and heptaethylene glycol monododecyl ether ($C_{12}E_7$) to elucidate the effect of Ca^{2+} on foam stability. The OPLS-AA force field was used. The authors found that LAS had a much larger Ca-binding number than SDS. They observed two preferred interaction distances between the calcium ion and the oxygen atoms of the surfactants: ∼0.23 and ∼0.45 nm. The results showed that LAS has many more interaction configurations at the shorter distance, while SDS has fewer. However, the reason for these two distances and how they are realized was not explained in ref 26. In another paper,[27] the authors compared the pure systems LAS and SDS with their mixture, which contained eight LAS and one SDS molecules under the same simulation conditions. It was discussed that the average binding number of Ca^{2+} to LAS was decreased and that to SDS was increased in the mixed system.

Zhao et al.[29] studied the effect of inorganic salt on two isomers of LAS, namely, 1C16 and 5C16, where the first number indicates the position of the benzene ring in the hydrocarbon chain. The studied systems contained 18 or 16 surfactant molecules, divided into two monolayers of 9 or 8 molecules, and the respective number of cations to neutralize the negative charges of the surfactants (Na^+ + Ca^{2+}, Na^+ + Mg^{2+}, or only Na^+). MD simulations with the COMPASS force field were performed for periods of 0.2 ns and analyzed. The authors discussed that the counterions (Na^+, Mg^{2+}, or Ca^{2+}) are distributed close to the air−water interface, screening the electrostatic repulsion between the charged surfactant head-groups. The effect of the counterions on the thickness of the interfacial water layer followed the series Ca^{2+} > Mg^{2+} > Na^+. This interfacial layer was quantified by calculating the thickness of the diffuse layer from the radial distribution functions (RDFs) between the sulfur atoms in the surfactant heads and the respective cations. The different behavior of Ca^{2+} and Mg^{2+} was explained with the smaller hydration radius of Ca^{2+}, which allowed these ions to penetrate into the hydration shell of the surfactant heads.

In all of these studies, similar types of model systems of surfactant molecules (two mirror-image monolayers formed by a small number of 10−20 molecules per system), separated by a thin aqueous phase (ca. 3−4 nm), were constructed. They were simulated for relatively short time periods, up to 4 ns. On the other hand, we found in our previous studies[33,34] that much longer production runs of ca. 100 ns are needed to reach equilibrium sampling even for small model systems. Moreover, the performed theoretical studies registered but could not explain the origin of the specific interactions between LAS and Ca^{2+} ions, which is well known from numerous experiments and has been quantified experimentally.[5]

Therefore, the major aim of the current study is to elucidate the molecular origin of this specific interaction and to clarify in detail the differences between LAS and SLES with respect to their interactions with the Na^+ and Ca^{2+} ions in adsorption layers. For this purpose, we performed much longer MD simulations of 150 ns. The influence of the surface concentration of the surfactant molecules on the cation binding and the effect of the used force fields (OPLS-AA vs CHARMM36) are studied, too. The origin of the specificity of binding is verified with additional MD simulations of model surfactant molecules, thus allowing us to check various possible hypotheses and to reach unambiguous conclusions. Combining extended MD trajectories of experiment-based models with the outcome from the model surfactants simulations, which are novel aspects of the work in the field, allowed us to provide a comprehensive molecular-level explanation of the origin of the specific effect of Ca^{2+} ions on the two sulfur-containing surfactants. These results provide clear guidelines for the synthesis of new calcium-tolerant, sulfate-free, and potentially more eco-friendly surfactant molecules for detergent applications.

In this paper, the effects of Ca^{2+} on diluted and dense monolayers of the separate surfactants (LAS or SLES) are compared first. The competition of cations binding to two coexisting LAS and SLES adsorption layers (diluted and dense) is presented next. This is followed by the simulations of the model surfactants (shown in the Supporting Information), the comparison of the force fields, and conclusions.

https://dx.doi.org/10.1021/acs.jpcb.0c06649
J. Phys. Chem. B 2020, 124, 10514−10528

METHODS AND MODELS

Two surfactants (LAS and SLES, Figure 1A) in the presence and absence of Ca^{2+} ions are studied. Even though commercial

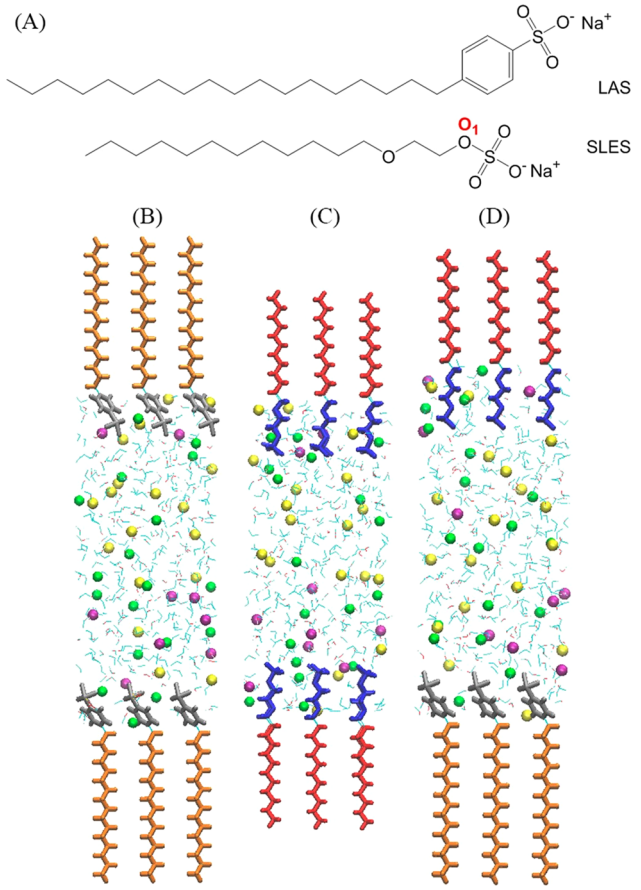

Figure 1. (A) Chemical structures of the surfactants studied. Side view of the initial models with (B) LAS, (C) SLES, and (D) asymmetric competitive. The hydrophobic tails are in red and orange (for SLES and LAS, respectively), the hydrophilic heads are in blue and gray (for SLES and LAS, respectively), water molecules are in cyan (H atoms) and red (O atoms), sodium ions are in green, calcium ions are in purple, and chloride ions are in yellow; the same color coding is used throughout the paper.

surfactant formulations often contain a mixture of linear and branched LAS representatives, the linear one is chosen for the present study for consistency with SLES and to be able to delineate only the influence of the type of counterions. Other differences, e.g., arising from spatial packing effects, are eliminated in this way. Three types of model systems (Figure 1), consisting of two monolayers at the vacuum−water interface, are constructed: (B) only SLES; (C) only LAS; and (D) "competitive" asymmetric LAS and SLES (two coexisting monolayers, each of them containing LAS or SLES only).

In all of these models, the effect of the addition of Ca^{2+} and the influence of the surface concentration of the surfactant molecules (expressed in terms of surface area per molecule) are monitored. Each monolayer contains nine surfactant molecules. The B3LYP/6−31*[35−39] optimized geometry of the single surfactant is used as the initial structure in the models. The molecule is replicated on the nodes of a regular two-dimensional (2D) square lattice by the software package VMD[40] so that the final spacing of the nine molecules corresponds to a predefined area per surfactant. The formed monolayer is then rotated by 180° and translated along z (the axis coinciding with the long molecular axis) at a distance of ≈3 nm (measured between the sulfur atoms of the heads) to obtain the mirror monolayer. Afterward, water molecules are added to fill the gaps between the surfactant heads and to fully solvate the latter. Then, sodium cations are randomly placed in the water layer to neutralize the negatively charged surfactant molecules. In the systems with Ca^{2+}, nine such cations are added randomly to the model described above, supplemented with chloride anions for neutralization.

In the asymmetric "competitive" model system, nine LAS molecules are adsorbed on one of the surfaces and nine SLES molecules on the other, thus allowing the two surfactant layers to "compete" for the adsorption of the Ca^{2+} and Na^{+} ions. In all constructed systems, the total number of surfactants is 18, neutralized by 18 sodium cations. When Ca^{2+} is added, 9 additional Ca^{2+} cations are neutralized by 18 Cl^{-} anions. To study the effect of surface concentration, the initial area per molecule was set to be either 0.81 or 0.40 nm^2, which corresponds to experimentally studied surface layers of LAS and SLES in the absence of Ca^{2+}.[5] At both surface areas, the number of all ions in the systems is kept the same. Only the number of water molecules is different. All used box sizes, number of water molecules, and number of all components in the systems studied are shown in Table S1 of the Supporting Information (SI). Periodic boundary conditions are applied in the lateral directions throughout the simulations, while along the z-axis (normal to the interface), about 13 nm of vacuum are added to discontinue the periodicity.

For comparison (see the Results and Discussion section), a separate MD simulation of bulk water (497 molecules) with one ion of each type (Na^{+} or Ca^{2+} neutralized by chloride anions) of 150 ns length is carried out to determine the number of water molecules in the unperturbed hydration shells of Na^{+} and Ca^{2+} ions.

Several additional models with different surfactant molecules are studied to check some of the hypotheses and to confirm all conclusions, obtained with the main systems. All of these additional models are constructed and analyzed following a protocol, identical to the one described above. Because the tendencies observed about the interactions of the molecules with the counterions are independent on the surface concentration, but more expressed for the denser monolayers, only dense layers are simulated and analyzed for the additional molecules.

The force-field OPLS-AA[41,42] is used for all ions, and the model SPC[43] is employed for the water molecules. Since OPLS-AA does not contain parameters for the sulfate and sulfonate fragments of the two surfactant molecules, the necessary values are adopted from the paper by Lopes et al.[42] for the sulfur-containing residues and from Velinova et al.[44] for the ether functional group in SLES. The atomic charges of the surfactants needed to calculate the electrostatic contribution to the energy are derived by applying the RESP procedure[45,46] where the charges are fit to the quantum mechanical electrostatic potential of each surfactant generated at the HF/6−31G* level for the B3LYP/6−31G* optimized geometries of the molecules.

The following MD computational procedure is applied to all systems studied: energy minimization of the initial configuration, heating to 298 K, relaxation for 1 ns, and production

https://dx.doi.org/10.1021/acs.jpcb.0c06649
J. Phys. Chem. B 2020, 124, 10514−10528

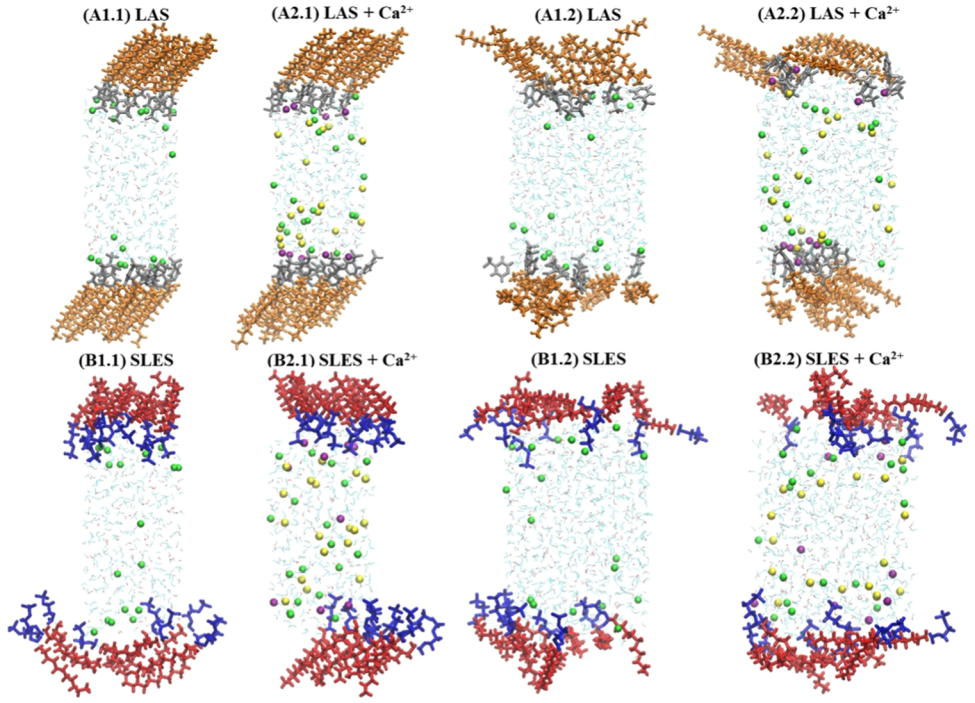

Figure 2. Snapshots of (A) LAS and (B) SLES for: (1.1) concentrated and (1.2) diluted layers without Ca^{2+}, (2.1) concentrated, and (2.2) diluted layers with Ca^{2+} after 150 ns of simulation.

runs with length of 150 ns. Leap-frog[47] is used to integrate the equations of motion with a time step of 1 fs. The molecular geometry of the surfactants is fully unrestrained. All MD simulations are done in the NVT ensemble to comply with the selected surface concentration. Constant temperature is maintained with the Nose−Hoover thermostat with a coupling constant of 0.4 ps. The Lennard-Jones potential is truncated at 9 Å with a switch function turned on at 7 Å. The electrostatic interactions are evaluated in the monopole approximation with the method PME;[48] the cutoff for the direct part of the sum is 9 Å with a switch function initiated at 7 Å. Equilibration of the systems is verified by monitoring the evolution of the total energy and temperature and of the RMSD of the surfactant coordinates. All of these parameters fluctuate around constant average values during the production runs (see Figure S1 for illustrative profiles), which confirms that equilibrium has been attained after 20 ns in all systems studied.

If not otherwise specified, the analyses presented below are performed for the last 50 ns of the simulation time (in some cases, divided into blocks), except for the parameters drawn as a function of time, which are presented for the entire trajectories. The frames are extracted at intervals of 0.5 ps. The program package GROMACS 5.0.6[49,50] is used for all simulations and for their analysis. VMD 1.9.1[40] is employed for visualization of the trajectories.

RESULTS AND DISCUSSION

The behavior of the molecules at the vacuum−water interface is studied by analyzing the density profiles of all components in the systems and the radial distribution functions (RDFs) between the surfactants and cations, and between the cations and water molecules to determine the hydration shells. The adsorption and desorption of the cations are quantified by tracking their *z*-coordinate as a function of time. The interaction energies are calculated from the RDFs between the charged heads of the surfactants and the counterions. The obtained results allow us to interpret the differences between the molecules of the two surfactants with respect to their interactions with the cations.

Effect of Ca^{2+} on Diluted and Concentrated Surfactant Monolayers of LAS and SLES. The effect of Ca^{2+} is first analyzed at the two surface areas, specified above, for pure LAS and SLES monolayers. In all systems, the number of Ca^{2+} ions is half the number of Na^{+} ions. The snapshots of the model systems at 150 ns of the MD simulations at both surface concentrations are shown in Figure 2A,B for LAS and SLES, respectively.

These snapshots illustrate that all Na^{+} cations are adsorbed on the LAS surfaces and almost all of them on the SLES surfaces when these are the only cations present. In the presence of Ca^{2+}, however, it is seen that only Ca^{2+} ions are adsorbed on the surfaces just in the LAS systems, while the Na^{+} ions are dispersed in the bulk. The same interaction pattern was registered previously in the MD simulations of an alkyl sulfonate monolayer.[14] In the SLES systems, no such qualitative difference in the behavior of the two cations is seen.

For both surfactants, the behavior of the cations does not depend strongly on the surface concentration. On the other hand, some differences are seen in the packing of the surfactant molecules—LAS is much more ordered on the surfaces than SLES, especially when calcium ions are present. In general, both molecules are more ordered at higher surface concentrations (in denser monolayers) due to the inherent steric restrictions in the adsorption layer.

Quantitative characterization of these visual observations is presented below by analyzing the mass density profiles normal to the interface in the period from 145 to 150 ns and the RDFs in the period from 100 to 150 ns.

Density Profiles. The density profiles of the different components (surfactant residues and ions) are calculated in

https://dx.doi.org/10.1021/acs.jpcb.0c06649
J. Phys. Chem. B 2020, 124, 10514−10528

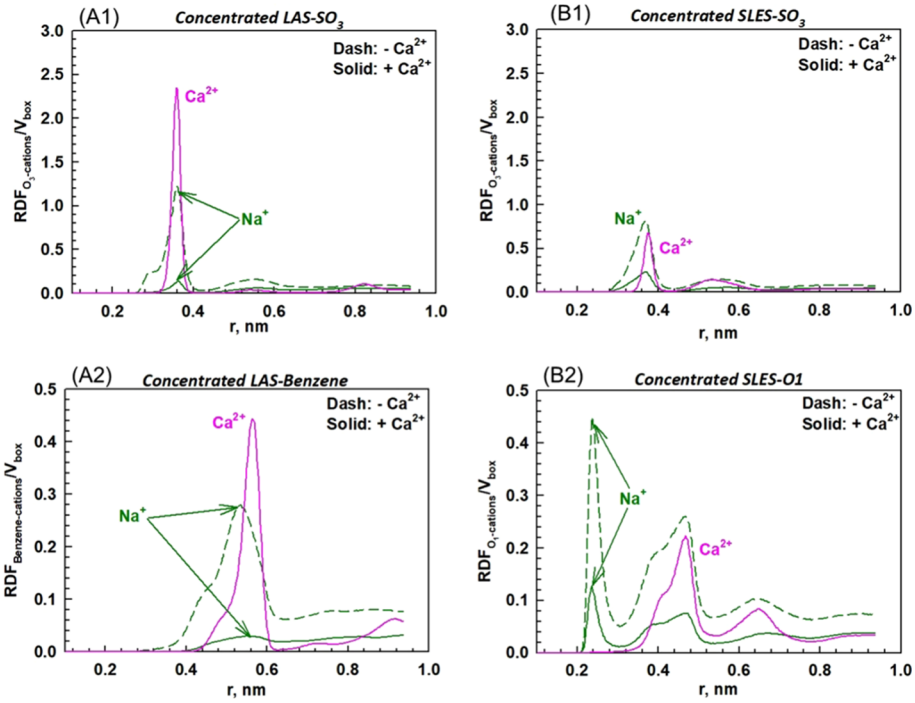

Figure 3. RDFs between the cations (green lines, Na^+; pink lines, Ca^{2+}) and the center of mass of (1) $-SO_3^-$ groups and (2) benzene ring/atom O1 (denoted in Figure 1) of (A) LAS and (B) SLES, respectively, in the concentrated systems in the presence (solid lines) and absence (dashed lines) of Ca^{2+}.

the presence and absence of Ca^{2+}. The results about the ions' density distribution in the concentrated systems, with and without Ca^{2+}, are presented in Figures S2−S4 of the SI. These data confirm the visual observations listed above and show that there are no free Na^+ ions in the bulk aqueous layer in the systems without calcium. The addition of Ca^{2+} does not affect significantly the position of the surfactants at the interface (Figures S2 and S3) but leads to displacement of the Na^+ ions from the adsorption layers of both types of surfactants. This effect results in distribution of the Na^+ ions in the bulk, but their density is higher near the surface with lower calcium density. This behavior is identical in all studied systems of single surfactants, irrespective of the surface concentration. Chloride anions are mobile during all simulations, with profiles mirroring those of Na^+.

It should be noted that clear differences in the Ca^{2+} density profiles are seen in LAS and SLES systems. The calcium density in the bulk is practically zero in LAS, but it is higher than zero in SLES. Also, the peak of Ca^{2+} in LAS is narrower than that in SLES. These results indicate that Ca^{2+} is bound more weakly to SLES, which allows the Ca^{2+} ions to traverse between the two surfaces. To examine the surfactant−ion interactions in more detail, several types of RDFs are compared below.

Radial Distribution Functions. The RDFs between the cations and the centers of mass (COMs) of the hydrophilic head-groups ($-SO_3$ group) or a specific residue (inner sulfate oxygen O1 for SLES and benzene ring for LAS) are calculated. The results for the concentrated surface layers of LAS and SLES, in the absence and presence of calcium, are compared in Figure 3. To be able to compare the results between surfactants and cations at the low and high surface concentrations studied, the raw data are scaled with respect to the simulation box volume, as shown in eq 1

$$\mathrm{RDF}_{\mathrm{scaled}} = \frac{\mathrm{RDF}}{V_{\mathrm{box}}} \tag{1}$$

The RDFs for diluted layers of LAS and SLES are presented in Figures S5.

In the LAS system, the RDF between the sulfonate group and both cations in the concentrated and diluted monolayers, exhibit one well-expressed peak at a distance of 0.36 nm (Figures 3A1 and S5A1). In the presence of calcium, the peak corresponding to the attraction between Na^+ ions and the sulfonate group considerably decreases in the concentrated system and practically disappears in the diluted one, which is due to the displacement of Na^+ by Ca^{2+} ions. However, the monolayer dilution does not affect the intensity of the RDF peak corresponding to Ca^{2+} binding (Figures 3A1 and S5A1). In other words, the surface concentration does not affect the interactions between the sulfonate group and Ca^{2+} while the dilution weakens the interaction with Na^+ ions. Similar effects are observed for the distances between the cations and the benzene ring (Figures 3A2 and S5A2).

In the pure SLES systems, the positions and the intensities of the RDF peaks are consistent with stronger interaction of the sulfate anion with Na^+ than with Ca^{2+} (Figures 3B1 and S5B1). One can assume that the larger hydrated Ca^{2+} ions cannot enter among the molecules in the adsorption layer while the smaller Na^+ ions can (see below). Hence, the binding of Na^+ to SLES is stronger than that of Ca^{2+}. In addition, non-negligible mobility of both cations between the two adsorption layers is registered, dissimilar to the LAS models. Unlike the interactions of the cations with LAS, those with SLES are significantly affected by the area per molecule in the adsorption layer. The peak intensity of the RDF between the sulfate oxygens and both cations decreases to less than half when the monolayer is diluted, while its position remains the same (Figures 3B1 and S5B1).

https://dx.doi.org/10.1021/acs.jpcb.0c06649
J. Phys. Chem. B 2020, 124, 10514−10528

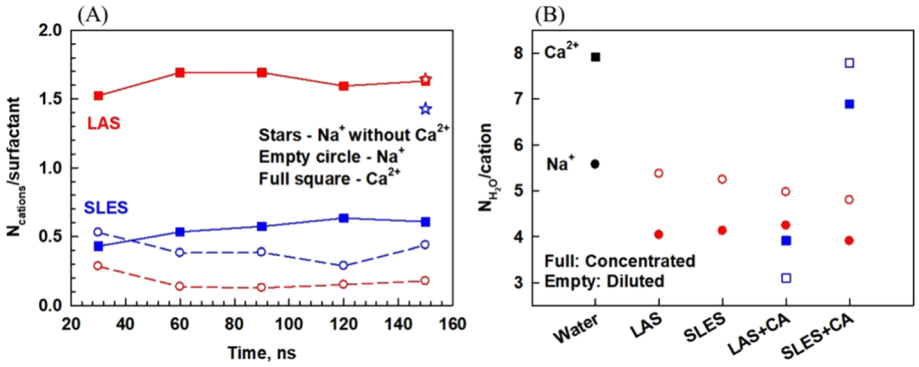

Figure 4. (A) Number of nearest ions (Na^+, empty circles in the presence of Ca^{2+} and empty stars in the absence of Ca^{2+}; Ca^{2+}, full squares) per surfactant (LAS, red symbols; SLES, blue symbols) as a function of time, in the concentrated systems of single LAS or SLES; data for the systems without Ca^{2+} are given only at 150 ns. (B) Number of water molecules surrounding the cations (Na^+, red circles; Ca^{2+}, blue squares) in the pure concentrated (full symbols) and diluted (empty symbols) systems; the black symbols are the reference number of water molecules in bulk solution, without any surfactant.

Interesting results are obtained about the interaction between the linking oxygen atom in SLES (O1 in Figure 1) and the cations. The most pronounced RDF peak is at a distance of 0.24 nm, which indicates that the Na^+ ions enter in between the SLES head-groups in the adsorption layer (Figure 3B2). This value is equal to the sum of the van der Waals radii of two hydrogen atoms, which means that there is no water between the surfactant molecules and the Na^+ ions, i.e., the latter have lost part of their hydration shell. In other words, the Na^+ ions successfully bind with the inner oxygen in SLES as well as interact with the outer oxygens. However, the interaction of Ca^{2+} with the inner oxygen is practically absent. Illustrations of a sodium ion located near the inner sulfate oxygens at a distance of 0.24 nm and the number of water molecules surrounding the cation are shown in Figure S6B1,B2 of the SI, respectively. This snapshot visually illustrates the observation that the Na^+ cations adsorbed among the SLES molecules lose partially their hydration shell (while the Ca^{2+} ion has remained outside). However, such conformations are realized in relatively short simulation times, only for several ns, indicating that their contribution to the average interaction energy is rather small.

To quantify the observed differences in the interactions between the various surfactants and cations, we averaged the RDF data over time intervals of 30 ns via eq 2 to calculate the number of bound counterions per surfactant molecule:

$$N_{\text{ions}} = 4\pi\rho_{\text{ion}} \int_{r_1}^{r_2} r^2 g_{\text{AB}} \mathrm{d}r \tag{2}$$

where r is the distance between the particles, ρ_{ion} is the mean ion number density, and g_{AB} is the radial distribution function between the respective particles. The integration is made over the first RDF peak only.

The number of bound cations as a function of the simulation time is shown in Figure 4A for both cations and both surfactants. One sees that the number of nearest Na^+ ions is about 1.5 for both LAS and SLES when Ca^{2+} is absent (star symbols in Figure 4A). The addition of Ca^{2+} significantly decreases the number of nearest sodium ions bound to each of the surfactants studied. Moreover, a substantial difference between the number of Ca^{2+} ions nearest to the surfactant heads is observed when the two surfactants are compared to each other, as discussed below.

For SLES in the presence of calcium, the number of cations from each type bound at a distance of 0.37 nm to SLES heads is almost the same (≈0.5 ion per surfactant molecule) and the total charge is approximately equal to the charge of the sodium ions in the absence of Ca^{2+}. A similar result is obtained about the number of cations in the second layer at a distance of 0.56 nm, and the sum of all surrounding cations in the presence and absence of calcium is equal to ≈3 per surfactant molecule. This latter number shows that the cations are shared between several surfactant head-groups, because the adsorption layers are electrically neutral. The number of Ca^{2+} is slightly higher than that of Na^+, which is probably due to the higher charge of Ca^{2+} ions, leading to stronger electrostatic attraction with the SLES head-group. Thus, we do not observe any sign for strong specific interaction between SLES and Ca^{2+} or Na^+ ions.

In contrast, the addition of calcium to the LAS system has a very significant effect. The number of bound Na^+ ions in the presence of Ca^{2+} drops almost to zero because the Na^+ ions are completely displaced from the adsorption layers by the Ca^{2+} ions. This result implies the presence of a strong specific interaction between the LAS molecules and Ca^{2+} ions. In addition, regular arrangement of the LAS molecules and Ca^{2+} bound to the LAS heads is observed, whereas no such regularity is seen in the ordering of SLES molecules with respect to the Ca^{2+} ions (Figure S7). A similar effect was reported by Yang et al.[26] when comparing the binding of Ca^{2+} to LAS and sodium dodecyl sulfate (SDS).

In our quest to clarify the molecular origin of the specific interaction between LAS and Ca^{2+}, we calculated also the average number of water molecules in the hydration shell of the cations in the bulk water solutions (without surfactant) and in the LAS and SLES systems. The number of nearest water molecules surrounding the cations was calculated from the corresponding RDFs during the last 50 ns of the simulations (Figure 4B). The obtained data for the hydration shells of the free cations are in very good agreement with the experimentally and theoretically determined data.[51,52] Our simulations clearly show that the cations bound to the surfactant molecules have fewer water molecules in their hydration shell, compared to their hydration in bulk water. The latter effect is particularly large for the Ca^{2+} ions interacting with LAS molecules—decrease from ca. 8 to 3−4 water molecules in the hydration shell of the Ca^{2+} ions bound to LAS. In all studied systems, the decrease is more pronounced

https://dx.doi.org/10.1021/acs.jpcb.0c06649
J. Phys. Chem. B 2020, 124, 10514−10528

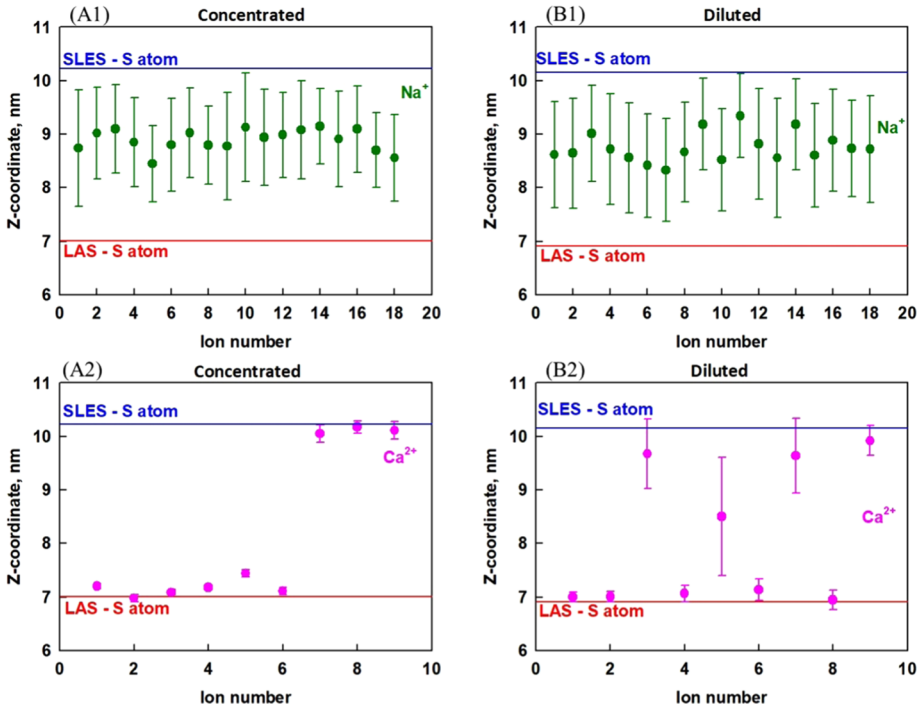

Figure 5. Average z-coordinates (with standard deviations) of all sodium ions (1, green circles) and calcium ions (2, pink circles) relative to the mean coordinates of the sulfur atoms in LAS (red line) and in SLES (blue line) monolayers in the (A) concentrated and (B) diluted mixed systems.

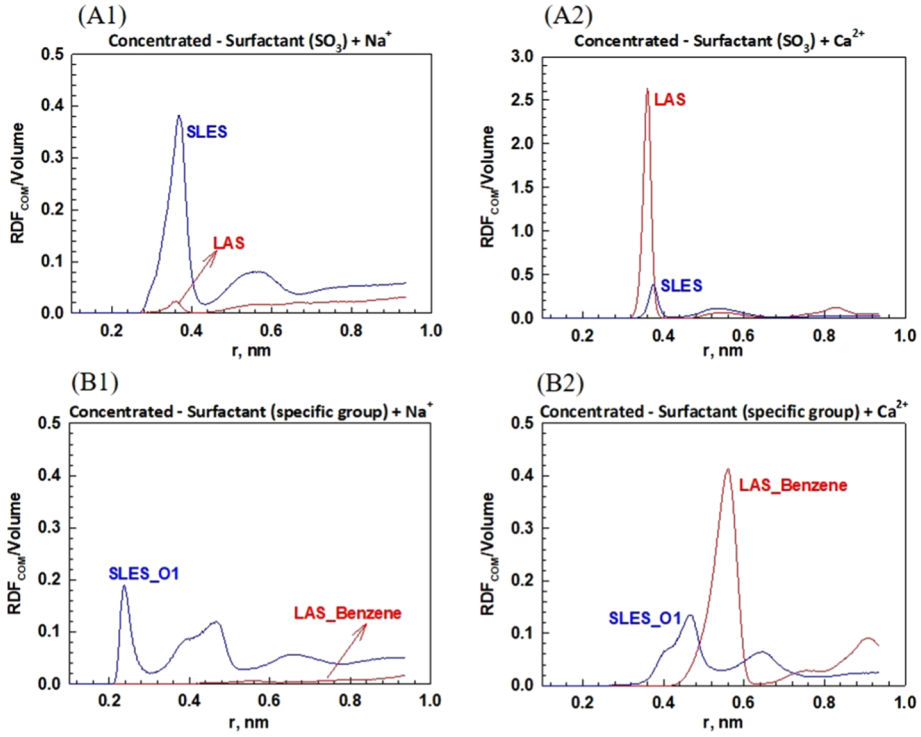

Figure 6. RDFs between the cations (1: Na^+, 2: Ca^{2+}) and (A) the SO_3 residue in the surfactant heads (LAS, red line; SLES, blue line) or (B) specific inner groups in the surfactant molecules: inner sulfate oxygen O1 in SLES and benzene ring in LAS; note the different ordinate scaling in A2.

in the concentrated monolayer than in the diluted one, except for the LAS + Ca^{2+} system, where the effect of surface concentration is negligible.

Competitive Cation Binding in Asymmetric Systems with Two Coexisting Adsorption Layers. To quantify better the observed differences, we studied the competitive interactions of the two counterions with coexisting surfactant monolayers of LAS and SLES. Model systems in the presence of Ca^{2+} and Na^+ ions were studied with both dilute and dense monolayers. The final configurations of the diluted and concentrated systems are compared in Figure S8 of the SI. One sees there that only Ca^{2+} ions are bound to the LAS

https://dx.doi.org/10.1021/acs.jpcb.0c06649
J. Phys. Chem. B 2020, 124, 10514−10528

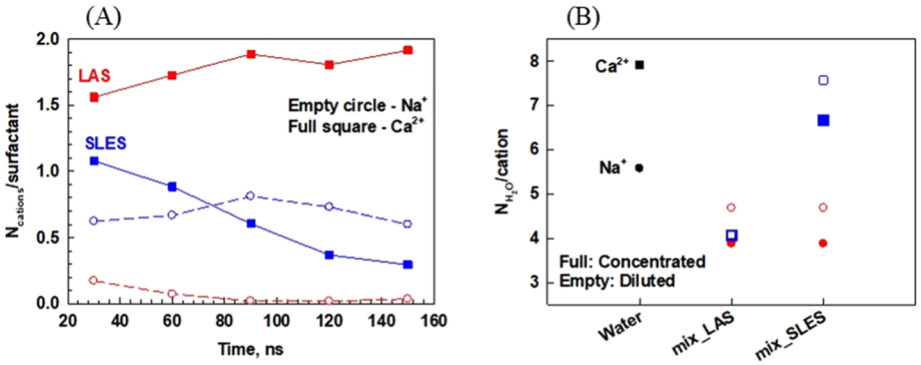

Figure 7. (A) Evolution of the number of counterions (Na^+, empty circles; Ca^{2+}, full squares) per surfactant molecule (LAS, red symbols; SLES, blue symbols) nearest to the $-SO_3$ or $-SO_4$ group in the concentrated asymmetric system. The most probable distances between the particles are 0.360 and 0.375 nm for LAS and SLES, respectively. (B) Number of water molecules surrounding the cations (red circles for Na^+, blue squares for Ca^{2+}) in asymmetric concentrated (full symbols) and diluted (empty symbols) systems; the black symbols are the number of solvating water molecules in the bulk water.

adsorption layer, while both cations interact with the SLES layer, which is an additional confirmation of the stronger affinity of the Ca^{2+} ions to LAS.

The visualized distribution of the molecular entities is quantified by the density profiles, presented and discussed in the SI (Figure S9). The main results and conclusions are similar to those obtained with systems containing single surfactants. The density profile of Ca^{2+} shows a much higher peak next to the LAS monolayer compared to the SLES monolayer. The six Ca^{2+} ions at the LAS surface seen in Figure S8 are adsorbed irreversibly in the time frame of the simulations. To check that the latter observation is not due to the initial position of the Ca^{2+} ions in the simulation box, additional simulations with a fixed initial position of the Ca^{2+} ions in the middle of the simulation box were run for the concentrated layer. The initial distance between Ca^{2+} and each surfactant at both surfaces was equal, and the final results about the Ca^{2+} density at the surfaces depend only on the relative strength of the interactions. The results (Figure S10) confirm that six Ca^{2+} ions are always bound to the nine LAS molecules in the layer, whereas the remaining three Ca^{2+} ions are bound to the SLES molecules, irrespective of their initial position in the box.

Unlike Ca^{2+}, sodium ions diffuse at all times across the whole water layer. These data are summarized for the last 50 ns of the simulation in Figure 5, as average values with standard deviations, drawn relative to a line denoting the average z-coordinate of the S atoms in the surfactant molecules, which is rather invariant along the trajectories. The error bars are a measure of the mobility of the ions. It is evident that the standard deviation of the average z-coordinate of the Na^+ ions is much larger than that of the Ca^{2+} ions, especially for the concentrated layers. In the diluted monolayers, the Ca^{2+} ions close to the SLES monolayer are much more mobile than those next to the LAS layer. This is another indication that the binding between SLES and Ca^{2+} is much weaker than that between LAS and Ca^{2+}.

To quantify the degree of binding between the surfactants and counterions, analysis of the RDFs and estimate of the potential of mean force (measure for the binding energy) are performed next.

Radial Distribution Functions. The scaled RDFs between the hydrophilic parts (polar and specific groups) of the surfactants and the counterions are shown in Figure 6. These data illustrate very well the affinity of the counterions to the respective surfactant. The RDF peak for the interaction of SLES with Na^+ is much higher than the peak for LAS and, oppositely, the peak for LAS with Ca^{2+} is much higher than that for SLES with Ca^{2+}. In other words, these simulations of coexisting layers confirm that Ca^{2+} has a strong preference for adsorption on the LAS monolayer, which leaves the SLES monolayer to be neutralized by the Na^+ counterions.

As already stated, these preferences of the counterions could be due to specific interactions with some fragments in the surfactant molecules (Figure 6B). In the asymmetric system, the RDF peak between benzene ring in LAS and Na^+ ion is practically missing and the RDF peak between O1 (SLES) and Ca^{2+} is much lower than the peak for O1 and Na^+. The positions of the peaks in all RDFs are the same as in the single-surfactant systems, which shows that these distances are characteristic for each ion−surfactant interaction. The peak for the interaction between sulfate oxygen O1 and Na^+ is at a shorter distance, compared to the distance between Na^+ and the outer oxygens, reflecting the ability of the Na^+ ions to immerse between the SLES heads at the interface via partial stripping of their hydration shells. On the other hand, for the LAS layer, the distance between the benzene ring and Ca^{2+} is longer than the distance between the Ca^{2+} and the sulfonate oxygens. The latter comparison indicates that (1) the RDF peak for benzene−Ca^{2+} is probably a byproduct of the preferred binding of Ca^{2+} ions to the sulfonate group and (2) no Ca^{2+} ions are immersed between the LAS heads.

The average number of nearest counterions to a surfactant is also calculated from the RDFs, and the data are presented as a function of time in Figure 7A. Qualitatively, the obtained results are very similar to those for the single-surfactant systems. In the asymmetric systems, the number of Na^+ and Ca^{2+} cations bound to SLES is almost equal and the number of Na^+ ions bound to LAS is practically zero. The number of Ca^{2+} ions bound to LAS is almost the same as that in the single-surfactant system. This means that each Ca^{2+} ion is in direct contact with (almost) two LAS molecules in the adsorption layer, while each SLES molecule binds approximately one positive charge, independently of the counterion type.

The hydration shells of the cations are compared in Figure 7B. One sees that the number of water molecules removed from the hydration shell of calcium significantly depends on the surfactant it interacts with. The interaction between LAS

https://dx.doi.org/10.1021/acs.jpcb.0c06649
J. Phys. Chem. B 2020, 124, 10514−10528

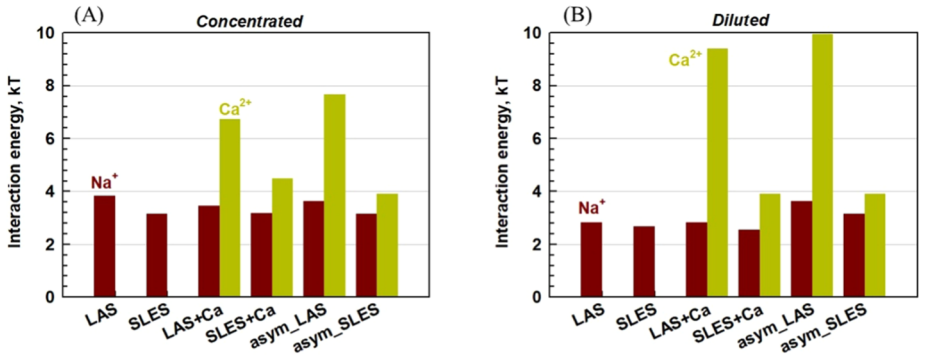

Figure 8. Interaction energies (eq 3) between the surfactants head-groups and the counterions (Na^+, dark red bars; Ca^{2+}, dark yellow bars): (A) concentrated and (B) diluted monolayers.

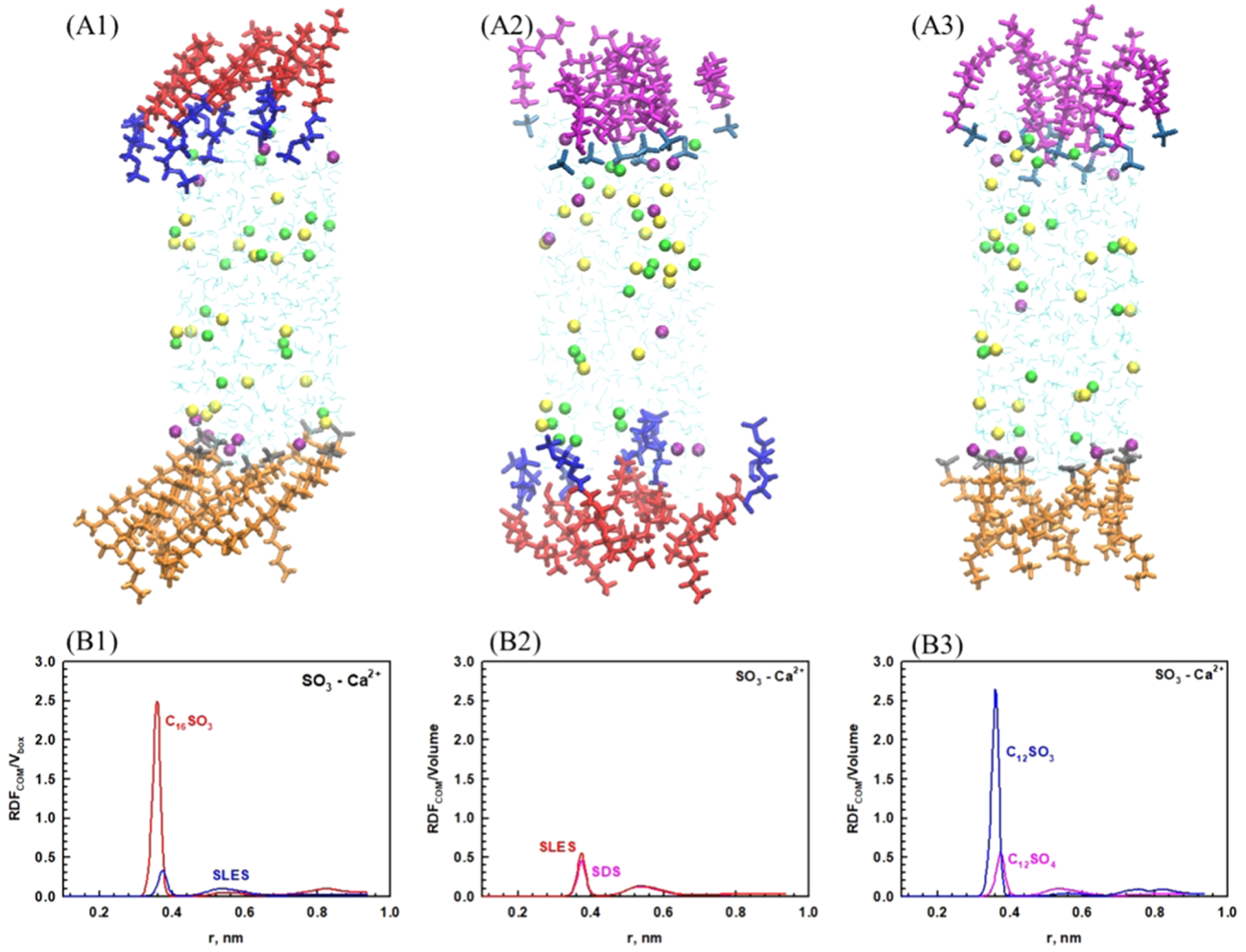

Figure 9. (A) Snapshots of the configurations at 150 ns from the simulation of the asymmetric systems: (1) SLES/$C_{16}SO_3$, (2) SDS/SLES, and (3) SDS/$C_{12}SO_3$; the modified surfactants are at the bottom surface in (1), at the top one in (2), and at both surfaces in (3). (B) RDFs between the SO_3 groups in each surfactant and Ca^{2+}.

and Ca^{2+} is not affected by the presence of SLES in this system—about four water molecules remain in the hydration shell of Ca^{2+} bound to LAS (from ca. 8 in bulk water). In contrast, Ca^{2+} stays surrounded by 7 ± 1 water molecules when it is near the SLES head-group.

In addition, the hydrogen bonds (HB) between the hydrophilic heads of the surfactants and the water molecules around them are analyzed and the results are presented in Figure S11 of the SI. We found that both surfactants form ≈5.6 HB with the water molecules in the absence of Ca^{2+} ions. This number is not affected for SLES, but it decreases significantly (almost 2-fold) for LAS in the presence of Ca^{2+}. The latter result is very important because it confirms that both Ca^{2+} and sulfonate head-group in LAS release water molecules upon binding to strengthen their interaction.

A quantitative appraisal of the interaction strength can be made by calculating the interaction energies from the radial distribution functions, $g(r)$, via eq 3

https://dx.doi.org/10.1021/acs.jpcb.0c06649
J. Phys. Chem. B 2020, 124, 10514−10528

$$w(r) = -kT \ln g(r) \quad \Delta w(r) = \ln \frac{g_{max}(r)}{g_{1st\_min}(r)} \tag{3}$$

where $w(r)$ is the potential of the mean force at a certain distance, $\Delta w(r)$ is the interaction energy in kT units, g_{max} is the RDF value corresponding to the first maximum, and g_{1st_min} is the RDF magnitude at the minimum after the first peak. The calculated data for all studied systems (single surfactant ± Ca^{2+} and asymmetric with Ca^{2+}) are compared in Figure 8.

One sees that the surface concentration has little influence on the interaction energies—all trends are the same for the diluted and the concentrated layers. It is evident that Na^+ cations bind with almost the same strength to any of the surfactants studied, independently of the presence of Ca^{2+}. This result shows that the interaction of Na^+ with the studied anionic surfactants is predominantly electrostatic, confirming the conclusions in ref 5.

On the other hand, there is a significant difference between the energies of Ca^{2+} binding to LAS and SLES. The energy is almost twice higher for LAS compared to SLES or to the interaction energy of LAS and Na^+. This result indicates that the interaction between Ca^{2+} and LAS is not purely electrostatic. To clarify unambiguously the molecular origin of this strong specific interaction, we performed additional simulations with designed model molecules, as described in the following section.

MD Simulations with Model Surfactants. The results from the simulations presented and discussed so far confirm the presence of a strong specific interaction between Ca^{2+} ions and LAS molecules, as reported experimentally.[5] The simulations show also that this interaction is related to significant reduction of the water molecules in the hydration shells of both the Ca^{2+} ions and the sulfonate head-group in LAS upon binding. They show also that the LAS molecules are more ordered in their adsorption layers, compared to SLES, and hint to possible contribution from the benzene ring present in the LAS molecules, which could enhance the molecular order via $\pi-\pi$ stacking interaction or could lead to strong ion-induced dipole interaction with Ca^{2+}, due to the very high polarizability of the aromatic groups. All of these effects interfere with each other and make it impossible to reveal the exact molecular mechanism which triggers them.

To make a crucial step further in this analysis, we defined several possible hypotheses about the origin of the specific interaction between Ca^{2+} and LAS, and checked them one by one with molecular simulations involving adsorption layers of other surfactant molecules with appropriately designed structures (Figure S12). These molecules were geometry-optimized, as described in the section Methods and Models, and simulated in asymmetric competitive models. These simulations were run only with concentrated surface layers in the presence of Ca^{2+} because this model system was found to be the most sensitive and discriminative with respect to the counterion binding. The calcium cations were positioned initially in the middle of the simulation box. All other simulation conditions are the same as for the asymmetric system LAS + SLES.

First, to check whether the benzene ring plays an important role in the LAS behavior, we made simulations in which we compared the properties of sodium hexadecylsulfonate ($C_{16}SO_3Na$) and SLES surfactant adsorption layers. The main results from this comparison are shown in Figure 9A1,B1, and they show clearly that the Ca^{2+} binding to $C_{16}SO_3$ head-group is much stronger compared to SLES. Thus, we conclude from this comparison that the benzene ring in the LAS molecules does not play any significant role for the observed specific interaction with Ca^{2+} ions.

Next, to clarify the role of the EO groups in the SLES molecules, we compared the layers of SLES ($C_{12}EOSO_4Na$) and SDS ($C_{12}SO_4Na$). These simulations showed that the interactions of the Na^+ and Ca^{2+} ions with these two surfactants were qualitatively similar, without signs of strong specific attraction with any of these molecules (see Figure 9A2,B2). The preferred distances between the sodium cation and the sulfate anion are the same (0.36 nm) in the two surfactants, which is in very good agreement with the value (0.35 nm) calculated theoretically from a phenomenological model.[53] The comparison between SLES and SDS clarifies that the EO groups in the SLES molecules do not affect very significantly the energy of Ca^{2+} interaction with SLES. The latter conclusion means that the main role of the bulky EO groups in suppressing the precipitation of SLES in hard water (compared to SDS or LAS) is to disturb the molecular packing in the solid calcium soaps of SLES, thus increasing the solubility constant of these soaps.

To check whether the longer hydrocarbon tail in LAS and in $C_{16}SO_3Na$ affects the interactions, we made additional simulations of coexisting layers of SDS ($C_{12}SO_4Na$) and sodium dodecyl sulfonate ($C_{12}SO_3Na$), where the difference between the surfactant molecules is the extra oxygen atom O1 in the sulfate group only. Again, we observe that the Ca^{2+} ions exhibit specific attraction only in the case of the sulfonate surfactant (Figure 9A3,B3), thus clarifying that the length of the alkyl chain and the molecular ordering in the adsorption layer, typical for the longer-chain surfactants, play a minor role in the specific interaction of the Ca^{2+} ions to the sulfonate molecules.

The final task in this analysis is to reveal the exact reason for the strong attraction of the Ca^{2+} ions with the sulfonate group. One reason could be that the charges of the terminal oxygen atoms in the surfactant heads are different and more negative in LAS, due to the redistribution of the charges between fewer oxygen atoms (three) compared to SLES (four). This difference is relatively small—of the order of 0.02 elementary charges—but it should be checked because it could affect the hydration properties of the sulfonate and sulfate groups. Therefore, we made additional simulations in which the oxygen charges in the sulfate group were taken to be the same as those in the sulfonate group in LAS. However, the simulations did not detect any significant effect of this change in the oxygen charges on the interaction of SLES with the Ca^{2+} ions (Figure S13). Therefore, the slightly different charges of the oxygen atoms in the sulfate and sulfonate groups do not explain the difference in Ca^{2+} binding. An additional simulation without Na^+ ions in the asymmetric LAS/SLES system was run to analyze the binding of SLES and Ca^{2+} in the absence of competitive counterions. Again, we found that much more Ca^{2+} ions are bound to LAS and those in the vicinity of the SLES layer are much more mobile (Figure S14).

On the other hand, in all surfactants containing a sulfonate group, in which the S atom is directly linked to the first C atom in the surfactant tail, we observe significant dehydration of the sulfonate group and of the Ca^{2+} ion—around four water molecules are released from the two interacting charged species upon their binding. In contrast, the dehydration of the

https://dx.doi.org/10.1021/acs.jpcb.0c06649
J. Phys. Chem. B 2020, 124, 10514−10528

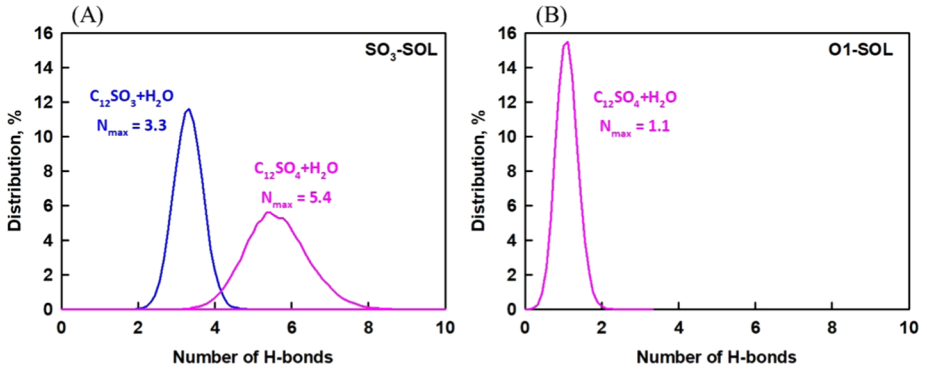

Figure 10. Distribution of the hydrogen bonds formed between water molecules and (A) SO_3 groups in $C_{12}SO_3$ and $C_{12}SO_4$ and (B) O1 atom in the sulfate group.

sulfate group and of the Ca^{2+} ion upon their binding is much less pronounced—only ca. 1.5 water molecules are released from the hydration shell of the counterion. This may be linked to the fact that it is known[54] that the sulfate anion prefers to hydrate at the interface as in the bulk—at the center of a spherical shell of water molecules.

The dehydration near LAS affects the mobility of Ca^{2+} as well. It is quantified by the *z*-coordinates of each cation averaged in the last 50 ns of the simulation (Figure S15). The large error bars indicate higher mobility of the ions in the vicinity of the sulfate-group-containing surfactants. This significant difference between the sulfonate and sulfate groups is observed for all surfactant molecules tested, including the molecules of dodecyl benzene sulfonate (LAS12) and dodecyl ethoxy sulfonate ($C_{12}EOSO_3$) (Figure S16). The respective results about the number of water molecules in the hydration shell of Ca^{2+}, the number of HBs between surfactant heads and water, and the interaction energies between surfactant heads and Ca^{2+} are summarized in Table S2 of the SI.

All of these combined results lead to the conclusion that there is a stronger hydrogen bonding between the water molecules and the sulfate anion, due to the extra oxygen atom O1, which precludes the direct binding of the sulfate group with the Ca^{2+} ions. Indeed, the average number of hydrogen bonds (HB) of the sulfate group with the neighboring water molecules is 6.5 HB, including 1.1 HB realized by the oxygen atom O1, whereas only 3.3 HB are observed on average for the sulfonate group (Figure 10). Due to this weaker interaction, the sulfonate group is able to strip water molecules, thus entering in a direct and stronger interaction with the partially dehydrated Ca^{2+} ions. We note that Ca^{2+} dehydration occurs in the interaction with the sulfonate group only and the latter does not strip water molecules when interacting with Na^+ ions. The reason may be the same as above because Na^+ is also characterized with bulk-like solvation at the air/water interface.[54] In addition, it has been found[55] that Ca^{2+} binds tightly two water molecules while Na^+ only 0.6. This leaves the two cations with comparable number (about 6) more loosely bound water molecules in the first hydration shell. Nevertheless, they are stripped differently in the vicinity of sulfate and sulfonate. These observations verify that the dehydration of the Ca^{2+} ion and of the sulfonate group is a specific collective process, involving a synchronized stripping of water molecules from both hydration shells. This is in line with the finding[55] that hydration/dehydration balance is very important for the interaction between ions in water.

Finally, we note that Ca^{2+} has stronger surfactant-ordering effect in the sulfonate surfactant systems compared to the sulfate surfactant systems. The specific interaction with the sulfonate groups leads to pronounced coordination of two to four neighboring surfactant molecules for each Ca^{2+} ion (Figure 11). No such strong coordination was observed with the sulfate surfactants, with or without EO groups.

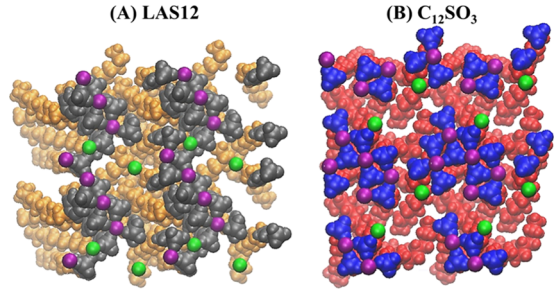

Figure 11. Illustration of the coordination effect of the adsorbed Ca^{2+} ions (purple balls) on monolayers of sulfonate surfactants: (A) LAS12: gray spheres and (B) $C_{12}SO_3$: blue spheres. The orange and red species are the hydrophobic tails of LAS12 and $C_{12}SO_3$, respectively.

Influence of the Force Field: OPLS-AA vs CHARMM36.

Upon survey of the literature about MD investigations of sulfur-containing anionic surfactants, we found a study[56] addressing the effect of the used force field (FF) on the structural properties of the molecular aggregates (micelles), composed of sodium dodecyl sulfate (SDS) molecules. Three FFs—OPLS-AA, CHARMM36, and GROMOS—were compared in NPT simulations.

Based on the observed Na^+ binding and the structure of the micellar aggregates, the authors concluded that CHARMM36 describes better than OPLS-AA the micellar systems studied in ref 56. Therefore, we decided to check the effect of the used force field on our systems. For this purpose, all simulations for the concentrated layers with LAS and SLES were repeated using CHARMM36, which contains all required parameters for the molecules studied by us.[32,57] The configurations of the systems calculated with the two force fields after 150 ns of MD simulation are compared in Figure 12.

Briefly, the main conclusions from the comparison of the two FFs are the following. The hydrophobic tails of the surfactants are more ordered when OPLS-AA is used, in agreement with Tang et al.[56] Still, the structuring in the LAS monolayers is more pronounced than that in SLES monolayers

https://dx.doi.org/10.1021/acs.jpcb.0c06649
J. Phys. Chem. B 2020, 124, 10514−10528

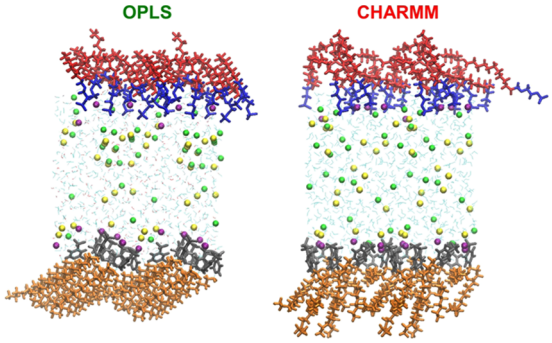

Figure 12. Snapshots of the asymmetric systems after 150 ns of simulation performed with OPLS-AA (left) and CHARMM36 (right). The periodic box is replicated along the *x*-axis to illustrate better the surfactants structuring.

also with CHARMM36. Therefore, no qualitative difference is found with respect to the surfactant ordering in the LAS and SLES layers when changing the FF.

With respect to the cations, both FFs predict the same general trend—Ca^{2+} ions displace Na^{+} ions from the adsorption layers by binding stronger to the surfactant heads. However, the cations are completely adsorbed close to the surfactants when OPLS-AA is used, whereas some Ca^{2+} ions remain in the bulk when CHARMM36 is employed (Figures S17 and S18). Furthermore, almost the same energy of interaction between Ca^{2+} and the two studied surfactants is obtained when CHARMM36 is used (Figure S19). Also, CHARMM36 yields comparable hydration of a given cation, independent of the surfactant. In particular, Ca^{2+} is observed to lose more than half of its hydration shell in both LAS and SLES systems (Figure S20).

The differences reported for the interaction of the Ca^{2+} ions with SLES when CHARMM36 is used are certainly due to the different protocols for parametrization in the two FFs. These dissimilarities could be caused by: (1) The different charges of the hydrophilic heads and (2) different Lennard-Jones parameters of the atoms in the surfactants and counterions (see the Supporting Information for the specific values). Note that equal empirically obtained charges are adopted for chemically similar residues in CHARMM36 (although they are optimized to reproduce water residue *ab initio* interaction energies of isolated clusters), while the ESP-based scheme recommended for OPLS-AA tries to capture the chemical specificity of the particular molecular environment, also taking into account the solvent effect by continuous solvation.

In our systems, the difference of atom charges may be important because the equalization of the atomic charges of the oxygen atoms in the sulfate and sulfonate groups leads to significant loss of the specificity of interaction with the calcium cations. The presence of the alkyl chains in surfactants could also affect the charges of differently located oxygen atoms, e.g., the internal and external oxygen atoms in the sulfate group. With regard to the van der Waals parameters, it should be mentioned that the hydration energies of the inorganic ions are the focus in the validation of OPLS-AA for both Na^{+} and Ca^{2+}. In CHARMM36, this target quantity is used only for Ca^{2+}, while the parameters for Na^{+} are tuned primarily to reproduce the interactions with oxygen atoms from lipid head-groups (carboxylates, phosphates, and esters), located at the gas–water interface. To compensate for this, the authors of the force field apply an *ad hoc* correction of the nonbonded interaction potential for Na^{+} and oxygen atoms with atom type O2L (used for sulfonate in our case).[58] Unfortunately, there is no such adjustment derived for oxygen atoms with type OG2P1 (employed for sulfate in the current study). It could be that this imbalance also adds to the less surfactant-specific performance of CHARMM36 in the current study. We tested this possibility by performing one additional simulation of the asymmetric concentrated system, using the atom type O2L also for the outer oxygen atoms of the sulfate group, i.e., by taking into account the *a posteriori* correction for both surfactants. The obtained results are almost the same (Figure S21), showing that the effect of the correction is minor in this case.

For the models studied here, the results provided above demonstrate that the balance between hydration and dispersion interactions is important for the specificity of binding of the Na^{+} and Ca^{2+} ions to LAS and SLES. This is probably one of the reasons for the better sensitivity of OPLS-AA to the variation of ions.

Concluding this discussion, the outcome obtained with OPLS-AA for our systems corresponds much better to the experimentally observed stronger and specific Ca^{2+} binding to LAS.[5] This comparison with the experiment, along with the physical reasoning provided above, convinced us to give a preference to the simulations made with OPLS-AA FF for the systems studied in the current article, although for more homogeneous systems, like those modeled in ref 56, CHARMM36 could provide a better description.

CONCLUSIONS

Fully atomistic molecular dynamics simulations of the adsorption layers of two anionic surfactants, widely used in detergency, are carried out under conditions mimicking the experimental ones. The modeled molecules, LAS and SLES, differ in their hydrophobic fragments and in their hydrophilic head-groups. Several model systems are constructed and simulated for 150 ns to compare the behavior of the surfactant molecules adsorbed at the gas–water interface. The focus of the study is on the surfactant interactions with the counterions Na^{+} and Ca^{2+}.

For both surfactants, qualitatively similar effects of the surface concentration and Ca^{2+} addition are observed. Decreasing the area per molecule in the adsorption layer leads to more ordered monolayers, and the Ca^{2+} ions displace the sodium ions from the monolayers. However, the observed effects of Ca^{2+} are much more pronounced for LAS compared to SLES. For SLES, the difference between the interaction energies with Na^{+} and Ca^{2+} ions is below 1 kT, whereas the interaction energy between LAS and Ca^{2+} is about 2 times higher than that between LAS and Na^{+} or SLES and Ca^{2+}.

We find also that Ca^{2+} reduces to one half its hydration shell (from ca. 8 to 4 water molecules) when it interacts with LAS, while it loses only one or two water molecules in the vicinity of SLES. The hydration of the sulfonate group in the LAS molecules is also decreased upon Ca^{2+} binding, while the hydration of SLES is not affected. In relation, the number of hydrogen bonds between the oxygen atoms in the surfactant heads and the water molecules decreases significantly when Ca^{2+} is bound to LAS. In contrast, there is no change in the number of H bonds between SLES and water when any of the two counterions, Ca^{2+} or Na^{+}, is bound. These differences highlight the preference for direct LAS–Ca^{2+} binding and confirm the conclusions from previous studies that this

https://dx.doi.org/10.1021/acs.jpcb.0c06649
J. Phys. Chem. B 2020, 124, 10514–10528

preference is reflected in relatively large specific energy of attraction.

Simulations with a series of specially designed model surfactants allowed us to clarify that the specific and most important feature of LAS is the lack of an inner oxygen atom, which is present in the sulfate group of SLES and other sulfate-based surfactants like SDS. This inner oxygen atom forms H bonds with the water molecules and thus holds them around the sulfate head-groups. As a result, both the sulfate group in SLES and the interacting Ca^{2+} ion remain hydrated, which leads to a much weaker, predominantly electrostatic interaction. The effects of the benzene ring and of the longer hydrocarbon tail in the LAS molecules are studied, but they turn out to have minor effects on the observed strong specific interaction between the sulfonate-based surfactants and Ca^{2+} ions.

All of these results and conclusions are in agreement with the experimental outcome reported in previous studies.[5] These conclusions provide important guidelines toward the understanding of the experimentally observed ion-binding selectivity of the two surfactants, in the presence of common monovalent and multivalent counterions, and suggest some ideas for a rational design of new surfactants with improved performance.

■ ASSOCIATED CONTENT

Supporting Information

The Supporting Information is available free of charge at https://pubs.acs.org/doi/10.1021/acs.jpcb.0c06649.

Description of the studied systems (Table S1); number of hydrating water molecules, number of hydrogen-bond SO_3−water, and SO_3−calcium interaction energies in the model surfactants simulations (Table S2); total energy, temperature, and RMSD of the surfactant coordinates as a function of simulation time (Figure S1); density profiles of the concentrated and diluted pure systems (Figures S2−S4); RDFs between the cations and functional groups of the surfactants in the pure systems (Figure S5); illustration of Na^+ and Ca^{2+} in the vicinity of the surfactant heads in the concentrated pure systems (Figure S6); illustration of the Ca^{2+} adsorbed beneath the monolayers in the pure system in the presence of Ca^{2+} (Figure S7); final snapshots of the simulations of the diluted and concentrated mixed system (Figure S8); density profiles in the concentrated and diluted mixed system (Figure S9); *z*-coordinates of all calcium cations as a function of time in the concentrated mixed systems with two initial configurations (Figure S10); distribution of the number of hydrogen bonds formed between SO_3 groups and water molecules (Figure S11); chemical structures of the molecules used as model surfactants (Figure S12); RDFs between the SLES heads and Ca^{2+} in the systems with the same charge of the oxygens in both molecules and in the original asymmetric system (Figure S13); z-coordinate of the Ca^{2+} in the system without Na^+ and RDFs between surfactant heads and Ca^{2+} in the system without added Na (Figure S14); averaged *z*-coordinates of the calcium cations in the model surfactants simulations (Figure S15); snapshots of the configurations at 150 ns of the simulation of the asymmetric systems and RDFs between the SO_3 groups in each surfactant and Ca^{2+} (Figure S16); density profiles of the surfactants and ions in the pure systems obtained with CHARMM36 (Figure S17); density profiles of the surfactants and ions in the mixed system obtained with CHARMM36 (Figure S18); RDFs between surfactant heads and cations in the pure and asymmetric systems obtained with CHARMM36 (Figure S19); number of water molecules surrounding the cations and interaction energies between surfactants head-groups and counterions obtained with CHARMM36 (Figure S20); and RDFs between surfactant heads and cations in the asymmetric system with identical CHARMM36 atom types for the outer oxygen atoms of LAS and SLES head-groups (Figure S21) (PDF)

■ AUTHOR INFORMATION

Corresponding Author

Anela Ivanova − *Department of Physical Chemistry Faculty of Chemistry and Pharmacy, University of Sofia, 1164 Sofia, Bulgaria;* orcid.org/0000-0001-6220-7961; Phone: + +35928161520; Email: aivanova@chem.uni-sofia.bg; Fax: + +35929625438

Authors

Fatmegyul Mustan − *Department of Chemical and Pharmaceutical Engineering, University of Sofia, 1164 Sofia, Bulgaria*

Slavka Tcholakova − *Department of Chemical and Pharmaceutical Engineering, University of Sofia, 1164 Sofia, Bulgaria;* orcid.org/0000-0001-8091-7529

Nikolai Denkov − *Department of Chemical and Pharmaceutical Engineering, University of Sofia, 1164 Sofia, Bulgaria;* orcid.org/0000-0003-1118-7635

Complete contact information is available at: https://pubs.acs.org/10.1021/acs.jpcb.0c06649

Notes

The authors declare no competing financial interest.

■ ACKNOWLEDGMENTS

Fatmegyul Mustan acknowledges the financial support from the program "Young scientists and Postdoctoral candidates" of the Bulgarian Ministry of Education and Science, MCD No. 577/17.08.2018. Part of this work was supported by computational time granted from the Greek Research & Technology Network (GRNET) on the National HPC facility ARIS under project "VI-SEEM", grant agreement no. 675121, application Surf_prop.

■ REFERENCES

(1) Alargova, R.; Petkov, J.; Petsev, D.; Ivanov, I. B.; Broze, G.; Mehreteab, A. Light scattering study of sodium dodecyl polyoxyethylene-2-sulfate micelles in the presence of multivalent counterions. *Langmuir* **1995**, *11*, 1530−1536.

(2) Kralchevsky, P. A.; Danov, K. D.; Broze, G.; Mehreteab, A. Thermodynamics of ionic surfactant adsorption with account for the counterion binding: Effect of salts of various valency. *Langmuir* **1999**, *15*, 2351−2365.

(3) Ma, J.-G.; Boyd, B. J.; Drummond, C. J. Positional isomers of linear sodium dodecylbenzene sulfonate: solubility, self-assembly, and air/water interfacial activity. *Langmuir* **2006**, *22*, 8646−8654.

(4) Tucker, I.; Penfold, J.; Thomas, R. K.; Dong, C. C.; Golding, S.; Gibson, C.; Grillo, I. The adsorption and self-assembly of mixtures of alkylbenzene sulfonate isomers and the role of divalent electrolyte. *Langmuir* **2011**, *27*, 6674−6682.

(5) Anachkov, S. E.; Tcholakova, S.; Dimitrova, D. T.; Denkov, N. D.; Subrahmaniam, N. P.; Bhunia, P. Adsorption of linear alkyl benzene sulfonates on oil−water interface: effects of Na^+, Mg^{2+} and Ca^{2+} ions. *Colloids Surf., A* **2015**, *466*, 18−27.
(6) Ivanova, V. I.; Stanimirova, R. D.; Danova, K. D.; Kralchevsky, P. A.; Petkov, J. T. Sulfonated methyl esters, linear alkylbenzene sulfonates and their mixed solutions: Micellization and effect of Ca^{2+} ions. *Colloids Surf., A* **2017**, *519*, 87−97.
(7) Matheson, K. L.; Cox, M. F.; Smith, D. L. Interactions between linear alkylbenzene sulfonates and water hardness ions. I. Effect of calcium ion on surfactant solubility and implications for detergency performance. *J. Am. Oil Chem. Soc.* **1985**, *62*, 1391−1396.
(8) Schweighofer, K. J.; Essmann, U.; Berkowitz, M. Simulation of sodium dodecyl sulfate at the water-vapor and water-carbon tetrachloride interfaces at low surface coverage. *J. Phys. Chem. B* **1997**, *101*, 3793−3799.
(9) Kuhn, H.; Rehage, H. Molecular dynamics computer simulations of surfactant monolayers: Monododecyl pentaethylene glycol at the surface between air and water. *J. Phys. Chem. B* **1999**, *103*, 8493−8501.
(10) Chanda, J.; Bandyopadhyay, S. Molecular dynamics study of a surfactant monolayer adsorbed at the air/water interface. *J. Chem. Theory Comput.* **2005**, *1*, 963−971.
(11) Jang, S. S.; Goddard, W. A. Structures and properties of Newton black films characterized using molecular dynamics simulations. *J. Phys. Chem. B* **2006**, *110*, 7992−8001.
(12) Yuan, S.; Ma, L.; Zhang, X.; Zheng, L. Molecular dynamics studies on monolayer of cetyltrimethylammonium bromide surfactant formed at the air/water interface. *Colloids Surf., A* **2006**, *289*, 1−9.
(13) Pang, J.; Wang, Y.; Xu, G.; Han, T.; et al. Molecular Dynamics Simulations of SDS, DTAB, and $C_{12}E_8$ Monolayers Adsorbed at the Air/Water Surface in the Presence of DSEP. *J. Phys. Chem. B* **2011**, *115*, 2518−2526.
(14) Yan, H.; Guo, X.-L.; Yuan, S.-L.; Liu, C.-B. Molecular dynamics study of the effect of calcium ions on the monolayer of SDC and SDSn surfactants at the vapor/liquid interface. *Langmuir* **2011**, *27*, 5762−5771.
(15) Smit, B. Molecular-dynamics simulations of amphiphilic molecules at a liquid-liquid interface. *Phys. Rev. A* **1988**, *37*, 3431−3433.
(16) Domínguez, H.; Rivera, M. Mixtures of sodium dodecyl sulfate/dodecanol at the air/water interface by computer simulations. *Langmuir* **2005**, *21*, 7257−7262.
(17) Li, C.; Zhang, T.; Ji, X.; Wang, Z.; Sun, S.; Hu, S. Effect of Ca^{2+}/Mg^{2+} on the stability of the foam system stabilized by ananionic surfactant: A molecular dynamics study. *Colloids Surf., A* **2016**, *489*, 423−432.
(18) Urbina-Villalba, G.; Landrove, R. M.; Guaregua, J. A. Molecular dynamics simulation of the interfacial behavior of a heptane/water system in the presence of nonylphenol triethoxylated surfactants. 1. Surface energy, surface entropy, and interaction energies as a function of temperature and surfactant concentration. *Langmuir* **1997**, *13*, 1644−1652.
(19) Zhang, S.; Zhu, P.; Sun, Y.; Yang, Y.; Cao, X.; Song, X.; Li, Y. Study of the molecular array behaviour of laurel alkanolamide at the oil−water interface and the high interfacial activity enhanced by an inherent synergistic effect. *RSC Adv.* **2014**, *4*, 41831−41837.
(20) Li, J.; Han, Y.; Qu, G.; Cheng, J.; Xue, C.; Gao, X.; Sun, T.; Ding, W. Molecular dynamics simulation of the aggregation behavior of N-dodecyl-N,N-dimethyl-3-ammonio-1- propanesulfonate/sodium dodecyl benzene sulfonate surfactant mixed system at oil/water interface. *Colloids Surf., A* **2017**, *531*, 73−80.
(21) Shi, W.-X.; Guo, H.-X. Structure, interfacial properties, and dynamics of the sodium alkyl sulfate type surfactant monolayer at the water/trichloroethylene interface: A molecular dynamics simulation study. *J. Phys. Chem. B* **2010**, *114*, 6365−6376.
(22) Burov, S. V.; Obrezkov, N. P.; Vanin, A. A.; Piotrovskaya, E. M. Molecular dynamic simulation of micellar solutions: A coarse-grain model. *Colloid J.* **2008**, *70*, 1−5.
(23) Jalili, S.; Akhavana, M. A coarse-grained molecular dynamics simulation of a sodium dodecyl sulfate micelle in aqueous solution. *Colloids Surf., A* **2009**, *352*, 99−102.
(24) Chen, Y.; Xu, G. Improvement of Ca^{2+}-tolerance by the introduction of EO groups for the anionic surfactants: Molecular dynamics simulation. *Colloids Surf., A* **2013**, *424*, 26−32.
(25) Li, C.; Li, Y.; Yuan, R.; Lv, W. Study of the microcharacter of ultrastable aqueous foam stabilized by a kind of flexible connecting bipolar-headed surfactant with existence of magnesium ion. *Langmuir* **2013**, *29*, 5418−5427.
(26) Yang, W.; Yang, X. Molecular dynamics study of the influence of calcium ions on foam stability. *J. Phys. Chem. B* **2010**, *114*, 10066−10074.
(27) Yang, W.; Yang, X. Molecular dynamics study of the foam stability of a mixed surfactant/water system with and without calcium ions. *J. Phys. Chem. B* **2011**, *115*, 4645−4653.
(28) Yang, W.; Wu, R.; Kong, B.; Zhang, X.; Yang, X. Molecular dynamics simulations of film rupture in water/surfactant systems. *J. Phys. Chem. B* **2009**, *113*, 8332−8338.
(29) Zhao, T.; Xu, G.; Yuan, S.; Chen, Y.; Yan, H. Molecular dynamics study of alkyl benzene sulfonate at air/water interface: Effect of inorganic salts. *J. Phys. Chem. B* **2010**, *114*, 5025−5033.
(30) Yuan, S.-M.; Yan, H.; Lv, K.; Liu, C.-B.; Yuan, S.-L. Surface behavior of a model surfactant: A theoretical simulation study. *J. Colloid Interface Sci.* **2010**, *348*, 159−166.
(31) Hu, X.; Li, Y.; He, X.; Li, C.; Li, Z.; Cao, X.; Xin, X.; Somasundaran, P. Structure behavior property relationship study of surfactants as foam stabilizers explored by experimental and molecular simulation approaches. *J. Phys. Chem. B* **2012**, *116*, 160−167.
(32) He, X.; Guvench, O.; MacKerell, A. D., Jr.; Klein, M. L. Atomistic simulation study of linear alkylbenzene sulfonates at the water/air interface. *J. Phys. Chem. B* **2010**, *114*, 9787−9794.
(33) Tsibranska, S.; Ivanova, A.; Tcholakova, S.; Denkov, N. Self-assembly of escin molecules at the air-water interface studied by molecular dynamics. *Langmuir* **2017**, *33*, 8330−8341.
(34) Mustan, F.; Ivanova, A.; Madjarova, G.; Tcholakova, S.; Denkov, N. Molecular dynamics simulation of the aggregation patterns in aqueous solutions of bile salts at physiological conditions. *J. Phys. Chem. B* **2015**, *119*, 15631−15643.
(35) Becke, A. D. Density-functional exchange-energy approximation with correct asymptotic behavior. *Phys. Rev. A* **1988**, *38*, 3098−3100.
(36) Becke, A. D. Density-functional thermochemistry. III. The role of exact exchange. *J. Chem. Phys.* **1993**, *98*, 5648−5652.
(37) Lee, C.; Yang, W.; Parr, R. G. Development of the Colle-Salvetti correlation-energy formula into a functional of the electron density. *Phys. Rev. B* **1988**, *37*, 785−789.
(38) Miehlich, B.; Savin, A.; Stoll, H.; Preuss, H. Results obtained with the correlation energy density functionals of Becke and Lee, Yang and Parr. *Chem. Phys. Lett.* **1989**, *157*, 200−206.
(39) Ditchfield, R.; Hehre, W. J.; Pople, J. A. Self-consistent molecular-orbital methods. IX. An extended Gaussian-type basis for molecular-orbital studies of organic molecules. *J. Chem. Phys.* **1971**, *54*, 724−728.
(40) Humphrey, W.; Dalke, A.; Schulten, K. VMD: Visual molecular dynamics. *J. Mol. Graphics Modell.* **1996**, *14*, 33−38.
(41) Jorgensen, W. L.; Madura, J. D.; Swenson, C. J. Optimized intermolecular potential functions for liquid hydrocarbons. *J. Am. Chem. Soc.* **1984**, *106*, 6638−6664.
(42) Lopes, J. N. C.; Pádua, A. A. H.; Shimizu, K. Molecular force field for ionic liquids IV: trialkylimidazolium and alkoxycarbonyl-imidazolium cations, alkylsulfonate and alkylsulfate anions. *J. Phys. Chem. B* **2008**, *112*, 5039−5046.
(43) Berendsen, H. J. C.; Postma, J. P. M.; van Gunsteren, W. F.; Hermans, J. Interaction models for water in relation to protein hydration. In *Intermolecular Forces*; Pullman, B., Ed.; D. Reidel Publ. Co: Dordrecht, 1981; pp 331−342.
(44) Velinova, M.; Tsoneva, Y.; Shushkov, P.; Ivanova, A.; Tadjer, A. Systematic derivation and testing of AMBER force field parameters

for fatty ethers from quantum mechanical calculations. *Progress in Theoretical Chemistry and Physics*; Springer: Dordrecht, 2012; Vol. *22*, pp 461−480.
(45) Bayly, C. I.; Cieplak, P.; Cornell, W. D.; Kollman, P. A. A. Well behaved electrostatic potential based method using charge restraints for deriving atomic charges − the RESP model. *J. Phys. Chem. A* **1993**, *97*, 10269−10280.
(46) Cieplak, P.; Cornell, W. D.; Bayly, C.; Kollman, P. A. Application of the multimolecule and multiconformational RESP methodology to biopolymers − charge derivation for DNA, RNA, and proteins. *J. Comput. Chem.* **1995**, *16*, 1357−1377.
(47) Hockney, R. W.; Goel, S. P.; Eastwood, J. Quiet high resolution computer models of a plasma. *J. Comput. Phys.* **1974**, *14*, 148−158.
(48) Darden, T.; York, D.; Pedersen, L. Particle mesh Ewald: An Nlog(N) method for Ewald sums in large systems. *J. Chem. Phys.* **1993**, *98*, 10089−10092.
(49) Abraham, M. J.; Murtola, T.; Schulz, R.; Páll, S.; Smith, J. C.; Hess, B.; Lindahl, E. GROMACS: High performance molecular simulations through multi-level parallelism from laptops to supercomputers. *Software X* **2015**, *1−2*, 19−25.
(50) Páll, S.; Abraham, M. J.; Kutzner, C.; Hess, B.; Lindahl, E. Tackling exascale software challenges in molecular dynamics simulations with GROMACS. In *Solving Software Challenges for Exascale*; Springer Int. Publ.: London, 2015; Vol. *8759*, pp 3−27.
(51) Marcus, Y. Ionic radii in aqueous solutions. *Chem. Rev.* **1988**, *88*, 1475−1498.
(52) Liu, C.; Min, F.; Liu, L.; Chen, J. Hydration properties of alkali and alkaline earth metal ions in aqueous solution: A molecular dynamics study. *Chem. Phys. Lett.* **2019**, *727*, 31−37.
(53) Koroleva, S.; Victorov, A. I. Modeling of the effects of ion specificity on the onset and growth of ionic micelles in a solution of simple salts. *Langmuir* **2014**, *30*, 3387−3396.
(54) Jungwirth, P.; Tobias, D. J. Specific ion effects at the air/water interface. *Chem. Rev.* **2006**, *106*, 1259−1281.
(55) Collins, K.; Neilson, G.; Enderby, J. Ions in water: Characterizing the forces that control chemical processes and biological structure. *Biophys. Chem.* **2007**, *128*, 95−104.
(56) Tang, X.; Koenig, P. H.; Larson, R. G. Molecular dynamics simulations of sodium dodecyl sulfate micelles in water − The effect of the force field. *J. Phys. Chem. B* **2014**, *118*, 3864−3880.
(57) Yu, W.; He, X.; Vanommeslaeghe, K.; MacKerell, A. D. Extension of the CHARMM general force field to sulfonyl-containing compounds and its utility in biomolecular simulations. *J. Comput. Chem.* **2012**, *33*, 2451−2468.
(58) Goh, G. B.; Eike, D. M.; Murch, B. P.; Brooks, C. L. Accurate modeling of ionic surfactants at high concentration. *J. Phys. Chem. B* **2015**, *119*, 6217−6224.

https://dx.doi.org/10.1021/acs.jpcb.0c06649
J. Phys. Chem. B 2020, 124, 10514−10528